



ELSEVIER

Journal of Magnetism and Magnetic Materials 191 (1999) 54–60

**J**ournal of  
**M**agnetism  
**and**  
**M**magnetic  
**materials**

# Suppression of magnetic coercivity in thin Ni films near the percolation threshold

Jin M. Choi<sup>a,c</sup>, Sihong Kim<sup>a,\*</sup>, Ivan K. Schuller<sup>a</sup>, Sun M. Paik<sup>b</sup>, C.N. Whang<sup>c</sup>

<sup>a</sup>Physics Department 0319, University of California - San Diego, La Jolla, CA 92093-0319, USA

<sup>b</sup>Physics Department, Kangwon National University, Choon-chun, Kangwon-do, South Korea

<sup>c</sup>Physics Department, Yonsei University, Shinchon-dong 134, Seodaemun-gu, Seoul, South Korea

Received 22 April 1998; received in revised form 8 August 1998

## Abstract

We have studied the behavior of magnetic coercivity  $H_c$ , across the geometric percolation in MBE grown epitaxial Ni films. By increasing a Cu buffer layer thickness, the morphology of Ni films changes from a collection of finite clusters to a single infinite cluster, while all other structural parameters remain constant.  $H_c$  drops rapidly near the geometric percolation threshold. Atomic Force Microscopy shows the presence of an infinite cluster with fractal dimension  $D_c \sim 1.9$ , in agreement with percolation theory. The suppression of  $H_c$  may be due to increased domain wall motion within the infinite cluster. © 1999 Published by Elsevier Science B.V. All rights reserved.

PACS: 75.70.-i; 75.60.-d; 68.55.Jk

Keywords: Magnetic coercivity; Thin Ni films; Cu buffer layer thickness; Infinite cluster

Magnetic thin films and multilayers have been studied extensively, not only because of their fundamental interest of magnetism, such as 2D magnetism [1], enhanced perpendicular magnetic anisotropy [2], new magnetic phases [3], Giant [4] and Colossal [5] magnetoresistance, etc., but also because they have potential applications in recording and sensor technologies. One of the most fundamental properties of ferromagnetic materials is the magnetic hysteresis loop. This can be characterized by the saturation magnetization  $M_s$ , the

remnance  $M_r$ , and the coercivity  $H_c$ . While  $M_s$  and  $M_r$  of a thin film have been thoroughly studied in basic research studies of thin films, the behavior of  $H_c$  has received much less attention [6]. The main reason is that  $H_c$  is strongly affected by many structural parameters including the morphology of the thin film and therefore it is not easy to design an experiment in which only one parameter is varied at a time. As a consequence, it is hard to attribute changes in  $H_c$  to specific parameters. In this work, we studied the magnetic hysteresis of epitaxial Ni films, whose morphology was changed by controlling an underlying Cu buffer layer thickness, while other structural parameters were fixed. This allows isolation of the effects of morphology on  $H_c$  from

\*Corresponding author. Tel.: 619-534-7161; fax: 619-534-0173; e-mail: sikim@ucsd.edu.

all other structural parameters.  $H_c$  is considerably suppressed near the two-dimensional percolation threshold, due to topological changes in the film morphology.

Percolation phenomena are found in many physical systems [7]. In metallic thin films, competition between substrate–adlayer cohesion and surface diffusion are responsible for morphological changes with increasing film thickness. Polycrystalline films, deposited on insulating substrates at high temperature, are typical examples [8–12]. The early growth stage of these metallic films is characterized by a homogeneous distribution of small islands. They grow in size through complete coalescence due to the high mobility of small droplets. Further increase of island size is limited by the substrate–adlayer cohesion, resulting in partial coalescence of neighboring droplets to form a percolating network. At the percolation threshold an infinite cluster [8,9] is formed, a fractal object of dimension  $< 2$ . Extensive electrical transport studies in such systems confirm the existence of many scaling laws [13,25]. However, the magnetic properties of percolating ferromagnetic thin films have received less attention in the published literature, except a transition from superparamagnetism to ferromagnetism, e.g., submonolayer films of Fe on W(1 1 0) [14]. Since magnetic properties are very sensitive to small variation in film microstructure, such as strain [15], they are hard to be established in mesoscopic systems. Studies of magnetic films which exhibit percolation may therefore be a fruitful area of research which may reveal new interesting phenomena.

We studied Ni films because their magnetic and structural properties are easily found in the literature. Especially, the magnetic properties of Ni films on Cu(0 0 1) can be found in recent publications [16] because of the perpendicular magnetic anisotropy (PMA) [17]. However, epitaxial Ni(1 1 1) on Cu(1 1 1) is more appropriate for our investigation. Because FCC metals grown along [1 1 1] direction usually have twinning structures due to equivalent stacking sequences, more diverse morphological change is expected than FCC(0 0 1) films. The complicated magnetic anisotropy energy due to strain found in Ni/Cu(0 0 1) would make Ni/Cu(1 1 1) a better system to study the morphological effect

although Ni/Cu(0 0 1) has been studied more extensively.

Epitaxial [1 1 1] oriented FCC Ni films were grown by molecular beam epitaxy (MBE) on single crystal  $\text{Al}_2\text{O}_3$  (0 0 0 1) substrates. Substrate preparation and metal deposition process were similar to those used in earlier work [18]. 10 Å of Pd seed layers were deposited first at 500°C. Cu buffer layers were subsequently deposited on the Pd seed layers at temperature 200°C for a wide range of thicknesses (200–1400 Å). 100 Å thick Ni layers were deposited on these Cu layers at 80°C to minimize diffusion at the Cu/Ni interface. Finally, 150 Å of Ag capping layers were evaporated to protect the Ni surface from oxidation in air and avoid exchange coupling [20] with NiO. The structure of the deposited films was characterized, in-situ, by RHEED, low energy electron diffraction (LEED), and Auger electron spectroscopy (AES), and, ex-situ, by X-ray diffraction (XRD), scanning electron microscopy (SEM), and atomic force microscopies (AFM).

The in-situ reflection high energy electron diffraction (RHEED) showed sharp streak patterns for 10 Å thick Pd seed layers, establishing the epitaxy between  $\text{Al}_2\text{O}_3$  [0 0 0 1] and FCC Pd[1 1 1] orientation. Fig. 1a shows the diffraction profile across the [0 0] RHEED streak with the electron beam along the [1  $\bar{1}$  0] direction in the FCC Cu(1 1 1) plane parallel to the film surface. The RHEED patterns were from Cu(1 1 1) surfaces at different layer thicknesses. As the Cu buffer layer thickness increases, the FWHM becomes smaller and eventually reaches the limit of the resolution in our data acquisition system [18]. The lateral size of the coherent crystalline domains of the Cu buffer layer increases with thickness. The lateral coherence lengths of our films will be discussed below in conjunction with AFM images.

Fig. 1b shows the XRD  $\theta$  scan of completed films, for a  $2\theta$  angle fixed at the Ni [1 1 1] Bragg reflection position. In contrast to RHEED profiles, all XRD data are identical regardless of buffer layer thicknesses (FWHM  $\sim 1^\circ$ ). FWHM of XRD  $\theta$  scan is very sensitive to both the growth and the post annealing temperature of Cu buffer layers. This implies that the crystallinity of the Ni films are constant for a wide range of lateral length scales.

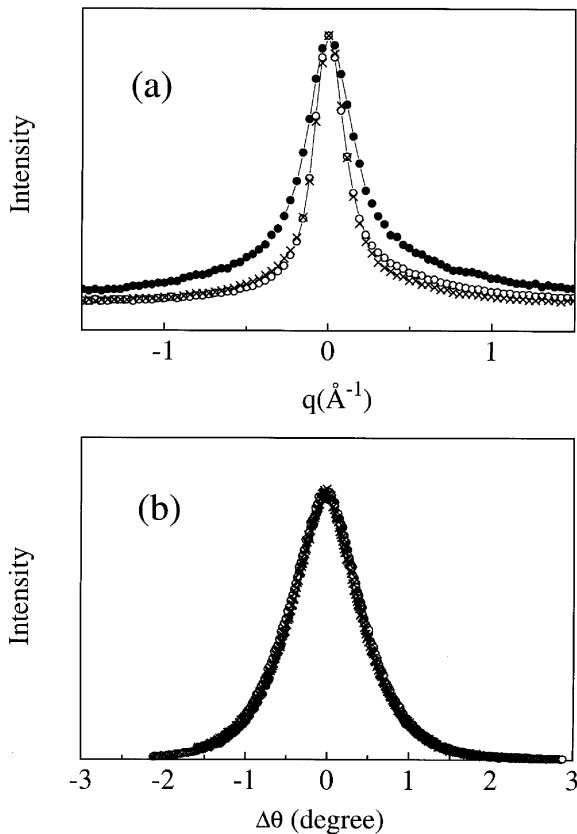


Fig. 1. (a) RHEED intensity profile across [0 0] streak taken at various thickness of Cu buffer layers. The electron beam is along the  $[1\bar{1}0]$  direction in the FCC Cu(1 1 1) surface in the plane of the film. (b) XRD  $\theta$  scan for a  $2\theta$  angle fixed at Ni[1 1 1] Bragg reflection for Ni films grown on various thickness Cu buffer layers. (•)  $d_{\text{Cu}} = 200$ , (○)  $d_{\text{Cu}} = 600$ , and (×)  $d_{\text{Cu}} = 1000$  Å.

This is particularly important in analyzing the magnetization data, because besides the changes in island size the variations in microstructure of the films are minimal. Thus the relationship between the morphological change and  $H_c$  can be extracted easily. Since the 100 Å Ni layers were deposited at low temperature, they do not have enough mobility to fill in the boundaries of Cu buffer matrix. Moreover, since Cu–Ni has small lattice mismatch, the thin Ni layers are expected to grow layer by layer on the surface of each Cu island, maintaining the similar island size. The same argument can be applied to the epitaxial Ag capping. Therefore, the

morphology of Cu/Ni, Ni/Ag, or Ag/air interface should not be significantly different. This is supported by conventional  $\theta$ – $2\theta$  scan XRD spectra. High angle XRD spectra show several well resolved finite size peaks around Ag[1 1 1] and Ni[1 1 1], corresponding to the thickness of Ag and Ni respectively [19]. There is little difference in XRD data among different samples, indicating similarity between Cu/Ni and Ni/Ag interfaces. The diffraction data show that the Ni films have uniform crystallinity and similar Cu/Ni and Ni/Ag interfaces, but significant changes in surface morphology.

Fig. 2 shows AFM images for various samples. The image size shown is fixed at  $10\ \mu\text{m}$ , although images were taken at various scan sizes (1– $80\ \mu\text{m}$ ). Although these images are taken on the final Ag surfaces, the Ni surface morphology should not be significantly different for the reasons mentioned above. The films with Cu layers thinner than 800 Å, consist of disconnected finite clusters. The average cluster size increases from 100 to 200 Å ( $d_{\text{Cu}} = 200$  Å) to several thousands Å's ( $d_{\text{Cu}} = 800$  Å). For films with Cu layers thicker than 800 Å, the morphological change is dominated by partial coalescence between neighboring islands, indicated by the elongated shape. Epitaxy does not appear to influence the surface morphology because the typical cluster size is many orders of magnitude larger than a lattice parameter. We should point out that the surface morphology of these epitaxial films is similar to those of polycrystalline Au, Pb, or In [8–10], but the average cluster size is much bigger, possibly, due to epitaxial growth. The cluster sizes are comparable to the magnetic length scales relevant here, which makes a study of the coercivity particularly interesting. A film with a 1000 Å Cu buffer is at the percolation threshold, while one with a 1100 Å Cu buffer passed the percolation point because very few finite clusters are found.

Fig. 3a shows coercivities determined from  $M$ – $H$  hysteresis measurements, with a magnetic field parallel to the film surface, using a SQUID magnetometer. The  $M$ – $H$  loops of all samples have a shape typical of a ferromagnetic film, with in-plane easy-axis due to shape anisotropy. The  $M_r$  to  $M_s$  ratio is similar for all samples as shown in

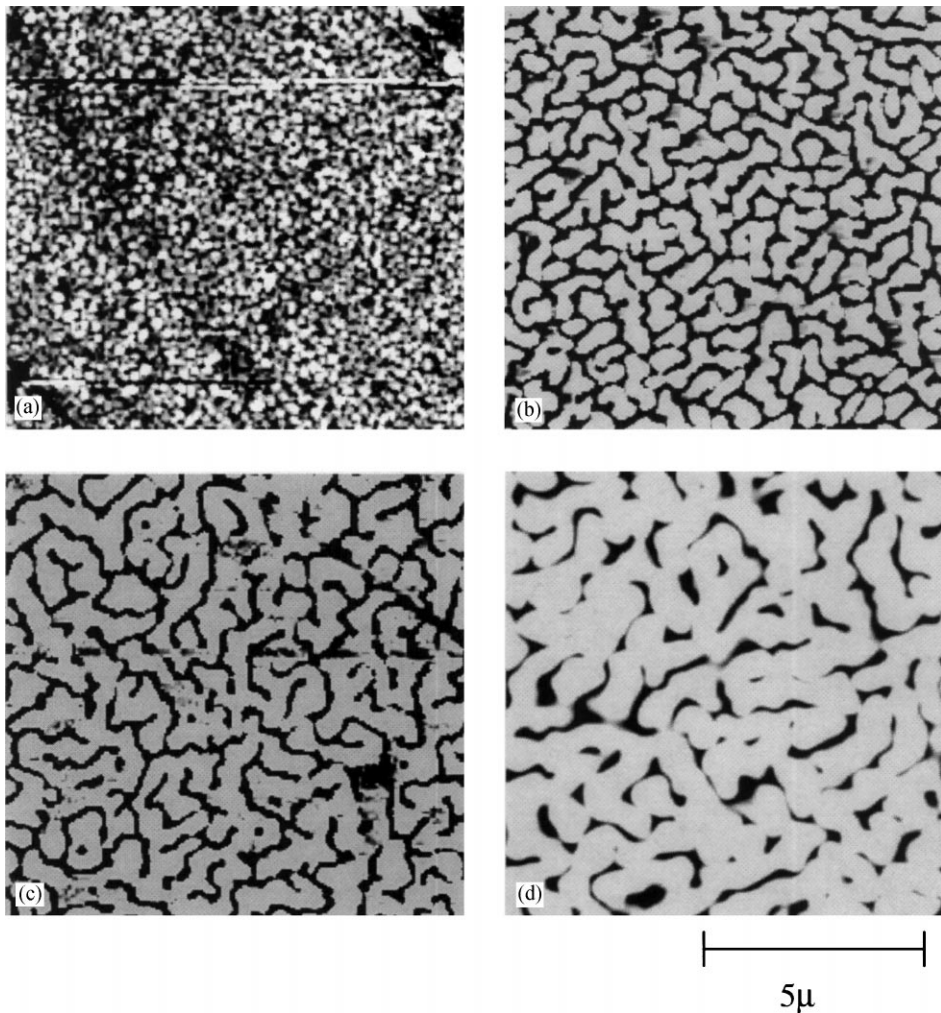


Fig. 2. AFM image of Ni films at various stage of morphological transformation. The underlying Cu buffer layer thickness is (a) 200 Å, (b) 900 Å, (c) 1000 Å, and (d) 1100 Å.

Fig. 3b. The  $M-H$  loops of all samples differ only in the magnitude of  $H_c$ . Since crystallinity, interface roughness, strain, etc., are similar for all samples, little variations are expected in the  $M-H$  loops except those induced by topological changes in the morphology.

$H_c$  shows a very interesting behavior. First, the magnitude of  $H_c$  is more than twice that of similarly prepared polycrystalline samples. Since epitaxial films have less defects,  $H_c$  is expected to be smaller. Second,  $H_c$  is independent of cluster size, in the range 100–200 Å ( $d_{Cu} = 200$  Å) to several thou-

sands Å's ( $d_{Cu} = 800$  Å). This is quite opposite to fine magnetic particles, where  $H_c$  is sensitive to the particle size [21]. Third,  $H_c$  shows a non-monotonic behavior as a function of cluster size although the surface morphology changes gradually towards a uniform, continuous film. A sudden drop in  $H_c$  near the percolation threshold is followed by a small maximum, and an eventual further decrease. These features are clearly resolved beyond experimental uncertainties. We tested the reproducibility of our data by making several duplicate samples. Not only the magnetic properties, but also

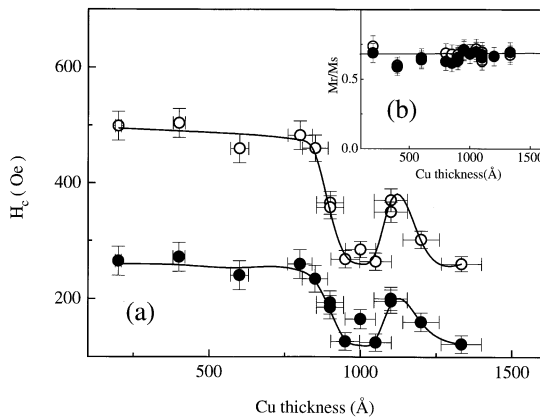


Fig. 3. (a) Coercivity of Ni films grown at various Cu buffer layer thickness. (b) Ratio of remnant  $M_r$  to saturation  $M_s$  magnetization of Ni films. (○) 10 K and (●) 300 K.

the structural characteristics, were reproducible within experimental error. The effect of in-plane anisotropy of the Ni films is smaller than the error bars shown in Fig. 3a. Since the magneto-crystal-line anisotropy constant of Ni is known to have a large temperature dependence [16,22],  $H_c$  might be expected to show a strong temperature dependence if this anomalous behavior would originate from it. The non-monotonic behavior of  $H_c$  is temperature independent. It is also unlikely that the surface and interface anisotropy of the films are responsible for this non-monotonic behavior because Ni films have the same thickness (100 Å) and the same Cu/Ni and Ni/Ag interfaces. Therefore this must be related to the topology of the Ni films, which affects domain wall motion in the magnetization reversal process.

To confirm that the  $H_c$  minimum coincides with the geometrical percolation threshold, AFM images of the samples around this minimum were analyzed, using the relatively simple method found in Ref. [9]. In this method, the mass density  $M(L)/L^2$  (where  $L$  is a probing length scale of a fractal system) exhibits a scaling behavior  $M(L) \sim L^{D_c}$ . Fig. 4 shows the results of such an analysis. The AFM images analyzed were digitized (512 × 512 pixels), and then an infinite object was isolated from the rest. This infinite object was examined whether it obeyed a scaling law. Below

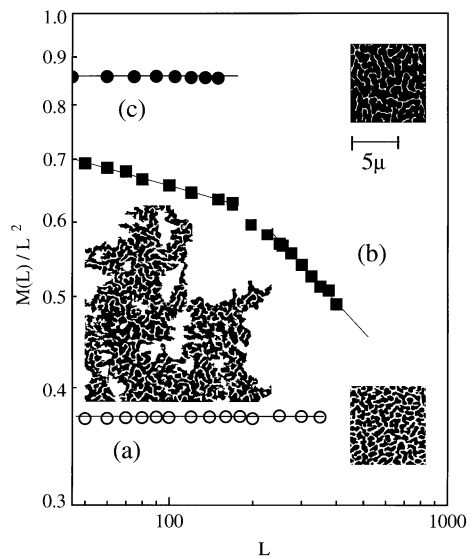


Fig. 4. Mass density as a function of probing length scale. (a) below, (b) near, and (c) above the percolation threshold.

the percolation point, the image is composed of finite clusters. The boundary of all clusters, a white image in Fig. 4a, is an infinite two-dimensional object. The mass density is constant independent of  $L$ . Note that the mass density shown in Fig. 4a, is not that of finite clusters, but the areal density of the voids between cluster boundaries. The constant value is nothing but  $(1 - \text{surface coverage})$ . Near the percolation point, the largest “infinite” cluster extended to all four boundaries of our maximum scan area (a black image in Fig. 4b). Initially, the mass density decreases with a power law (exponent  $\sim 0.08 \pm 0.02$ ), corresponding to  $D_c \sim 1.92 \pm 0.02$ . This agrees with the fractal dimension published in Ref. [8,9]. As  $L$  increases further, another power law was revealed (exponent  $\sim 0.32 \pm 0.08$ ), corresponding to  $D_c \sim 1.68 \pm 0.08$ , close to the fractal dimension of a backbone structure in Ref. [9]. This cross-over appears when  $L$  is close to the typical hole size. As  $L$  increases, the mass density analysis reflects more of a backbone structure because contribution from boundary regions becomes significant. From this analysis, it is clear that  $H_c$  drops rapidly near the two-dimensional geometrical percolation point. Above the percolation point, an infinite cluster becomes a two-dimensional object again (Fig. 4c).

There are three distinct regions in the data of Fig. 3; (I) high  $H_c$  below percolation, (II)  $H_c$  minimum at percolation, and (III) small maximum after percolation. The films in region (I) are composed of small clusters. The distance between boundaries is large enough that direct exchange interaction among clusters is unlikely. The size of most clusters is small enough that domain wall formation within clusters is unlikely, although pinning of the domain wall at the boundary is possible. In such systems, independent abrupt magnetization reversal of each cluster is expected [23]. On the other hand, the films in region (II) have a percolation cluster, composed of a backbone and dangling ends. This cluster has an unusually long perimeter due to a highly ramified structure. If the magnetization reversal initiates by releasing (or creating) domain walls at the external perimeter, a percolating cluster would have a higher chance than a small one to begin the process. In addition, the domain wall could move easily through the backbone. Therefore, lower  $H_c$  is expected. The films in region (III) shows increased length of the internal perimeter surrounding the holes within a cluster. Since the Ni films are only 100 Å thick, domain walls parallel to the film surface are unlikely. Therefore, one-dimensional domain walls propagating through the two-dimensional surface would be an appropriate description of the reversal process. Moving the domain wall across internal voids may be difficult for the same reason that three-dimensional inclusions pin domain walls. However, the length of the internal perimeter will decrease as the surface coverage becomes unity. Thus, a small  $H_c$  maximum would result due to changing density of pinning sites. A recent report on the propagation of magnetic domains in Ni/Cu(0 0 1) films [24], using magneto-optical Kerr effect (MOKE) microscopy, supports our interpretation. They showed the magnetic domain images, displaying the pinning of the domain wall by the scratches in the films. Although they have little information on the morphology, they speculate an interdependence between crystallographic structure of the buffer layer and the magnetic properties of the overlayer. In their work, the magnetic domain images and the magnetization relaxation experiments indicate that magnetization reversal occurs through domain nucleation and

domain-wall propagation. In addition, recently, big  $H_c$  has been reported on ultra thin Fe (1.5 ml) on W(1 1 0) [15]. Although their films are under severe stress and the size of sesquilayers are much smaller than ours, big  $H_c$  was attributed to the novel domain wall pinning. Therefore, it is unlikely that our data simply reflect the changes in the magnetic anisotropy energy (MAE) either by the interface strain, or the corner atom configuration in cluster, although MAE is important in other properties, such as, spin reorientation transition of Ni/Cu(0 0 1) [16].

In summary, we have shown that the hysteresis loop of Ni films exhibits a non-monotonic behavior in the coercivity, which is related to topological changes in the morphology. Since other structural parameters are constant, they are clearly not responsible for this behavior. To the best of our knowledge, this is the first report that percolation influences the magnetic coercivity of ferromagnetic thin films. A simple argument of non-interacting single domain clusters has been proposed as a possible explanation. Direct measurements of the magnetic domains are necessary to have a better understanding of this phenomenon. More detailed quantitative analysis, such as a micro-magnetic calculation which include realistic morphology, would be also desirable.

We thank Bernhard Knigge for assistance in AFM measurement and Jose Martin and Yvan Jaccard for SEM measurement. We also thank H. Suhl for useful conversations. This work is supported by US Department of Energy. J.M. Choi thanks financial support in part by the KOSEF through the Atomic Scale Surface Science Research Center at Yonsei University.

## References

- [1] R.F.C. Farrow (Ed.), *Magnetism and Structure in Systems of Reduced Dimension*, Plenum Press, New York, 1993.
- [2] J.G. Gay, R. Richter, *Phys. Rev. Lett.* 56 (1986) 2728 and references therein.
- [3] T. Asada, S. Blügel, *Phys. Rev. Lett.* 79 (1997) 507 and references therein.
- [4] M.N. Baibich, J.M. Broto, A. Fert, F. Nguyen Van Dau, F. Petroff, *Phys. Rev. Lett.* 61 (1988) 2472.

- [5] R. von Helmolt, J. Wecker, B. Holzapfel, L. Schultz, K. Samwer, *Phys. Rev. Lett.* 71 (1993) 2331.
- [6] G. Bochi, C.A. Ballentine, H.E. Inglefield, C.V. Thomson, R.C. O'Handley, H.J. Hug, B. Stiefel, A. Moser, H.J. Güntherodt, *Phys. Rev. B* 52 (1995) 7311.
- [7] D. Stauffer, *Introduction to Percolation Theory*, Taylor & Francis, London, 1994.
- [8] R.F. Voss, R.B. Laibowitz, E.I. Alessandrini, *Phys. Rev. Lett.* 49 (1982) 1441.
- [9] A. Kapitulnik, G. Deutscher, *Phys. Rev. Lett.* 49 (1982) 1444.
- [10] X. Yu, P.M. Duxbury, G. Jeffer, M.A. Dubson, *Phys. Rev. B* 44 (1991) 13163.
- [11] F. Family, P. Meakin, *Phys. Rev. Lett.* 61 (1988) 428.
- [12] W.T. Elam, S.A. Wolf, J. Sprague, D.U. Gubser, D. Van Vechten, G.L. Barz Jr., *Phys. Rev. Lett.* 54 (1985) 701.
- [13] R.B. Laibowitz, Y. Gefen, *Phys. Rev. Lett.* 53 (1984) 380.
- [14] H.J. Elmers, J. Hauschild, H. Höche, U. Gradmann, H. Bethge, D. Heuer, U. Köhler, *Phys. Rev. Lett.* 73 (1994) 898.
- [15] D. Sander, R. Skomski, C. Schmidhals, A. Enders, J. Kirschner, *Phys. Rev. Lett.* 77 (1996) 2566.
- [16] M. Farle, B. Mirwald-Schulz, A.N. Anisimov, W. Platow, K. Baberschke, *Phys. Rev. B* 55 (1997) 3708.
- [17] G. Bochi, C.A. Ballentine, H.E. Inglefield, C.V. Thomson, R.C. O'Handley, *Phys. Rev. B* 53 (1996) R1729.
- [18] S. Kim, H. Suhl, I.K. Schuller, *Phys. Rev. Lett.* 78 (1997) 322.
- [19] E.E. Fullerton, I.K. Schuller, H. Vanderstraeten, Y. Bruynseraede, *Phys. Rev. B* 45 (1992) 9292.
- [20] W.H. Meiklejohn, C.P. Bean, *Phys. Rev.* 105 (1957) 904.
- [21] B.D. Cullity, *Introduction to Magnetic Materials*, Ch. 11, Addison-Wesley, Reading, MA, 1972.
- [22] C. Kittel, *Rev. Mod. Phys.* 21 (1949) 541.
- [23] W. Wernsdorfer, E.B. Orozco, K. Hasselbach, A. Benoit, B. Barbara, N. Demoncey, A. Loiseau, H. Pascard, D. Maily, *Phys. Rev. Lett.* 78 (1997) 1791.
- [24] P. Rosenbusch, J. Lee, G. Lauhoff, J.A.C. Bland, *J. Magn. Mater.* 172 (1997) 19.
- [25] G. Deutscher, A. Kapitulnik, M.L. Rappaport, in: G. Deutscher, R. Zallen, J. Adler (Eds.), *Percolation Structures and Process*, AIP, New York, 1983.